Inorg. Chem. **2007**, *46*, 5459–5461

Tridecanuclear and Docosanuclear Manganese Phosphonate Clusters with Slow Magnetic Relaxation

Yun-Sheng Ma, You Song, Yi-Zhi Li, and Li-Min Zheng*

State Key Laboratory of Coordination Chemistry, Coordination Chemistry Institute, School of Chemistry and Chemical Engineering, Nanjing University, Nanjing 210093, P. R. China

Received January 21, 2007

Two novel mixed-valent manganese phosphonate clusters $[Mn^{II}Mn^{III}_{12}O_6(OH)_6(O_3PC_6H_{11})_{10}(py)_6]$ (**1**) and $[Mn^{II}_4Mn^{III}_{18}O_{12}(O_3PC_6H_{11})_8(O_2CCH_3)_{22}(H_2O)_6(py)_2]$ (**2**) are reported in this paper. Complex **1** is the first carboxylate-free manganese phosphonate cluster. While compound **2** appears to be the largest manganese cluster thus far that contains phosphonate ligand. Both show slow magnetic relaxation behaviors.

Single-molecule magnets (SMMs) have gained considerable attention in recent years.[1] It is well-known that a high-spin ground state (*S*) and a negative uniaxial anisotropy (*D*) are required for molecules to exhibit SMM behavior. Manganese clusters are attractive candidates in this respect because they often display relatively large spin ground states, and large negative D values may arise from the presence of Jahn−Teller (JT) distorted Mn^{III} ions.[2] Although carboxylates are most commonly used as the peripheral ligands, the phosphonate ligands with tetrahedral $\{CPO_3\}$ groups have proven to be efficient in the construction of new manganese clusters in the presence of coligands.[3−6] Winpenny et al. reported the largest manganese phosphonate cages of $[Mn^{III}_{20-x}Mn^{II}_x]$ ($x = 2$, 4, 6) so far where the carboxylate appears as the coligand. All three show unusual SMM behaviors with a high-spin ground state (19 ± 1, 14 ± 1, and 11 ± 1, respectively) and high coercivity.[3] It is found that a slight modification of the phosphonate ligand[4] and the presence of different base[6] would result in different structures of clusters and, hence, different properties. In this paper, we report two novel mixed-valent Mn_{13} and Mn_{22} phosphonate cages obtained by using different solvents, namely, $[Mn^{II}Mn^{III}_{12}O_6(OH)_6(O_3PC_6H_{11})_{10}(py)_6]$ (**1**) and $[Mn^{II}_4Mn^{III}_{18}O_{12}(O_3PC_6H_{11})_8(O_2CCH_3)_{22}(H_2O)_6(py)_2]$ (**2**). Slow magnetic relaxation behaviors are observed in both compounds at low temperature.

The reaction of $C_6H_{11}PO_3H_2$ and $[Mn_3O(O_2CCH_3)_6(py)_3]ClO_4$ in py in a molar ratio of 2:1 gave a dark brown solution. Dark block-shaped crystals of **1**·8py·3H_2O formed in 65% yield by diffusion of Et_2O into the filtrate. The reaction of equal molar amounts of $C_6H_{11}PO_3H_2$ and $[Mn_3O(O_2CCH_3)_6(py)_3]ClO_4$ in CH_2Cl_2 gave a dark brown solution from which compound **2**·12H_2O was obtained in 55% yield.[7]

Single-crystal X-ray diffraction studies[8] reveal that complex **1**·8py·3H_2O crystallizes in a triclinic space group $P\bar{1}$. The molecule is centrosymmetric with the Mn^{II} ion lying on the inversion center (Figure 1).

The core structure may be dissected into three layers with an ABA arrangement. Layer A consists of three Mn^{III} ions (Mn1, Mn3, Mn5) joined together by one μ_2-OH^- and three O−P−O units; layer B consists of a Mn^{III}_6 hexagon (Mn2, Mn4, Mn6, and their symmetry-related partners) with a Mn^{II} ion (Mn7) in the center that can be described as six edge-sharing partial cubane units. Such a $[Mn^{II}Mn^{III}_6O_{12}]$ core may

* To whom correspondence should be addressed. E-mail: lmzheng@netra.nju.edu.cn.

(1) (a) Winpenny, R. E. P. *Adv. Inorg. Chem.* **2001**, *52*, 1. (b) Gatteschi, D.; Sessoli, R. *Angew. Chem., Int. Ed.* **2003**, *42*, 268. (c) Aromí, G.; Brechin, E. K. *Struct. Bonding* **2006**, *122*, 1.

(2) For example, see: (a) Sessoli, R.; Gatteschi, D.; Caneschi, A.; Novak, M. A. *Nature* **1993**, *365*, 141. (b) Ruiz, D.; Sun, Z.; Albela, B.; Folting, K.; Ribas, J.; Christou, G.; Hendrickson, D. N. *Angew. Chem., Int. Ed.* **1998**, *37*, 300. (c) Coronado, E.; Forment-Aliaga, A.; Gaita-Ariño, A.; Giménez-Saiz, C.; Romero, F. M.; Wernsdorfer, W. *Angew. Chem., Int. Ed.* **2004**, *43*, 6152. (d) Tasiopoulos, A. T.; Vinslava, A.; Wernsdorfer, W.; Abboud, K. A.; Christou, G. *Angew. Chem., Int. Ed.* **2004**, *43*, 2117. (e) Brechin, E. K.; Soler, M.; Christou, G.; Helliwell, M.; Teat, S. J.; Wernsdorfer, W. *Chem. Commun.* **2003**, 1276. (f) Wernsdorfer, W.; Aliaga-Alcalde, N.; Hendrickson, D. N.; Christou, G. *Nature* **2002**, *416*, 406. (g) Ako, A. M.; Hewitt, I. J.; Mereacre, V.; Clérac, R.; Wernsdorfer, W.; Anson, C. E.; Powell, A. K. *Angew. Chem., Int. Ed.* **2006**, *45*, 4926.

(3) Maheswaran, S.; Chastanet, G.; Teat, S. J.; Mallah, T.; Sessoli, R.; Wernsdorfer, W.; Winpenny, R. E. P. *Angew. Chem., Int. Ed.* **2005**, *44*, 5044.

(4) (a) Yao, H.-C.; Li, Y.-Z.; Song, Y.; Ma, Y.-S.; Zheng, L.-M.; Xin, X.-Q. *Inorg. Chem.* **2006**, *45*, 59. (b) Ma, Y.-S.; Yao, H.-C.; Hua, W.-J.; Li, S.-H.; Li, Y.-Z.; Zheng, L.-M. *Inorg. Chim. Acta* **2007**, *360*, 1645.

(5) Shanmugam, M.; Chastanet, G.; Sessoli, R.; Mallah, T.; Wernsdorfer, W.; Winpenny, R. E. P. *J. Mater. Chem.* **2006**, *16*, 2576.

(6) Shanmugam, M.; Shanmugam, M.; Chastanet, G.; Mallah, T.; Sessoli, R.; Teat, S. J.; Timco, G. A.; Winpenny, R. E. P. *Chem.—Eur. J.* **2006**, *12*, 8777.

(7) Elemental Anal. Calcd (%) for **1**·8py·3H_2O ($C_{130}H_{194}N_{14}O_{45}P_{10}Mn_{13}$): C, 42.23; H, 5.29; N, 5.30. Found: C, 42.31; H, 5.41; N, 5.25. IR (KBr, cm^{-1}): ν 3446.80 (m), 2929.42 (s), 2852.16 (s), 1600.51 (m), 1447.71 (s), 1121.47 (vs), 1067.33 (vs), 1034.56 (vs), 989.84 (vs), 700.12 (m), 555.74 (s), 498.21 (m). Elemental Anal. Calcd (%) for **2**·12H_2O ($C_{102}H_{200}N_2O_{98}P_8Mn_{22}$): C, 27.35; H, 4.50; N, 0.63. Found: C, 27.38; H, 4.42; N, 0.57. IR (KBr, cm^{-1}): ν 3420.22 (s), 2929.60 (s), 2852.0.3 (m), 1544.14 (vs), 1436.93 (vs), 1345.94 (m), 1276.64 (w), 1212.20 (w), 1124.02 (s), 1103.44 (s), 1039.34 (s), 985.31 (s), 918.73 (m), 855.45 (w), 674.28 (s), 619.75 (s), 570.86 (s), 493.80 (m), 468.30 (m), 420.72 (m).

10.1021/ic070104b CCC: $37.00
Published on Web 06/06/2007

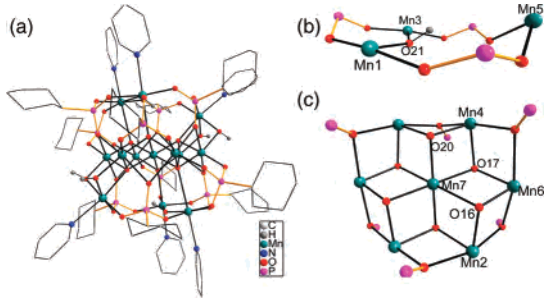

Figure 1. (a) Molecular structure of **1**. Layers (b) A and (c) B of the inorganic core of **1**. Hydrogen atoms except those in the hydroxy groups are omitted for clarity.

be compared with those in $[Mn_7(OH)_3Cl_3(hmp)_9]^{2+}$,[9] $[Mn_7(OMe)_{12}(dbm)_6]$,[10] and other larger clusters, such as $[Mn_{13}]$,[11] $[Mn_{19}]$,[12] $[Mn_{21}]$,[13] $[Mn_{25}]$,[14] and $[Mn_{26}]$.[15] Layers A and B are connected by a combination of oxide, hydroxide, and phosphonate ligands. The outer coordination shell is occupied by phosphonate ligands and terminal pyridine ligands (Figure 1). The metal oxidation states and the protonation level of O^{2-} and OH^- are established by the Mn and O bond valence sum calculations and the detection of Mn^{III} JT elongation axes. Although the JT axes are not parallel, there is a net contribution of anisotropy from the single Mn^{III} ions (Supporting Information). Ten phosphonate ligands in this structure adopt two bridging modes: six in η^1,η^1,η^2-μ_4 mode and four in η^1,η^1,η^1-μ_3 mode (Scheme 1).

Complex **2**·12H_2O also crystallizes in a triclinic space group $P\bar{1}$. The molecule, however, shows a wheel-like structure in which two equivalent cages of $[Mn^{III}_9O_6(O_3PC_6H_{11})_2(O_2CCH_3)_8(H_2O)]$ are connected by two pairs of Mn^{II} ions through phosphonate and carboxylate bridges (Figure 2). The core structure of $[Mn^{III}_9O_6(O_3PC_6H_{11})_2(O_2CCH_3)_8(H_2O)]$ contains a $[Mn^{III}_7O_4]$ subunit consisting of two $[Mn^{III}_4O_2]$ "butterfly" units (Mn1, Mn2, Mn3, Mn5 and Mn2, Mn4, Mn6, Mn8, respectively) fused by sharing a "body" Mn atom (Mn2). The resultant $[Mn^{III}_3O_4]$ base is almost planar with an Mn1−Mn2−Mn6 angle of 176.5°. Pairs of the "wing-tip" Mn atoms (Mn5, Mn8 and Mn3, Mn4) of the $[Mn^{III}_7O_4]$ subunit are further linked to two Mn^{III} ions (Mn10, Mn7) through two μ_3-O^{2-} (O5, O6), forming a $[Mn^{III}_9O_6]$ cluster. This cluster is capped by two phosphonate ligands via the coordination of the phosphonate oxygen atoms with the Mn atoms, resulting in a cage. Two such cages are fused by two pairs of Mn^{II} ions (Mn9, Mn11) through the phosphonate oxygens (O13, O16, O17) and carboxylate bridges, generating a wheel-like cluster with a rectangular cavity in the middle. The coordinated water molecules locate within this cavity (Figure 2).

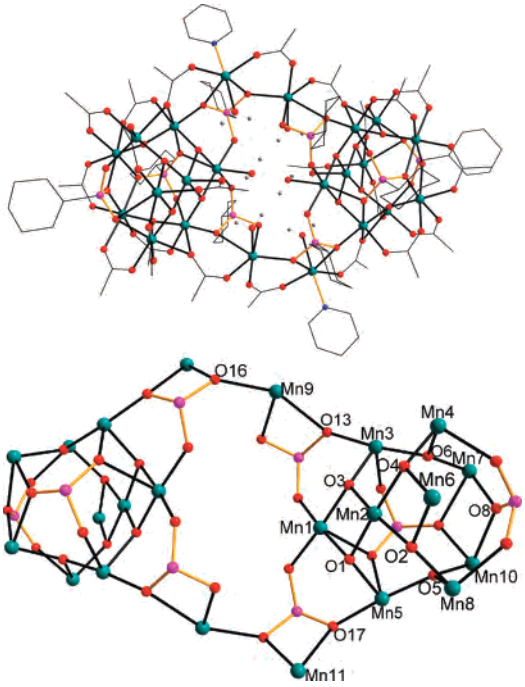

Figure 2. Molecular structure of **2** (top). Inorganic core of **2** (bottom). Hydrogen atoms except those in H_2O are omitted for clarity.

Scheme 1

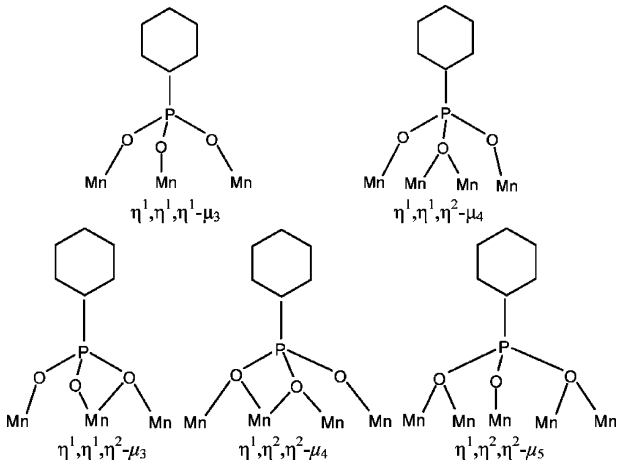

The phosphonate ligands coordinate to three, four, or five Mn atoms in four modes: η^1,η^1,η^2-μ_3, η^1,η^2,η^2-μ_4, η^1,η^1,η^2-μ_4, and η^1,η^2,η^2-μ_5 (Scheme 1). The oxidation states of the Mn atoms are established by bond valence sum calculations. All Mn^{III}, except Mn2 and Mn6, are six-coordinated with a distorted octahedral geometry. Mn2 and Mn6 are five-

(8) Crystal data for **1**·8py·3H_2O: triclinic, space group $P\bar{1}$, a = 15.685(3) Å, b = 18.024(3) Å, c = 18.425(3) Å, α = 64.790(3)°, β = 89.451(4)°, γ = 65.596(3)°, V = 4203.4(13) Å^3, Z = 1, M_r = 3696.91, ρ = 1.460 g cm^{-1}, $F(000)$ = 1907, μ(Mo Kα) = 1.111 mm^{-1}. Crystal data for **2**·12H_2O: triclinic, space group $P\bar{1}$, a = 15.4116(11) Å, b = 18.2450(13) Å, c = 20.7028(15) Å, α = 89.7340(10)°, β = 71.6370(10)°, γ = 71.1540(10)°, V = 5198.0(6) Å^3, Z = 1, M_r = 4479.08, ρ = 1.431 g cm^{-1}, $F(000)$ = 2280, μ(Mo Kα) = 1.428 mm^{-1}. The data collection was carried on a Bruker Smart Apex CCD diffractometer using graphite-monochromatized Mo Kα radiation (λ = 0.71073 Å). The structure was solved by direct methods and refined on F^2 by full-matrix least-squares using SHELXTL,[20] converging at R_1 = 0.0535, R_2 = 0.1129 for **1**·8py·3H_2O and R_1 = 0.0568, R_2 = 0.1157 for **2**·12H_2O, respectively.
(9) Harden, N. C.; Bolcar, M. A.; Wernsdorfer, W.; Abboud, K. A.; Streib, W. E.; Christou, G. *Inorg. Chem.* **2003**, *42*, 7067.
(10) Abbati, G. L.; Cornia, A.; Fabretti, A. C.; Caneschi, A.; Gatteschi, D. *Inorg. Chem.* **1998**, *37*, 3759.
(11) Jones, L. F.; Raftery, J.; Teat, S. J.; Collison, D.; Brechin, E. K. *Polyhedron* **2005**, *24*, 2443.
(12) Pohl, I. A. M.; Westin, L. G.; Kritkos, M. *Eur.—Chem. J.* **2001**, *7*, 3439.
(13) Brockman, J. T.; Huffman, J. C.; Christou, G. *Angew. Chem., Int. Ed.* **2002**, *41*, 2506.
(14) Murugesu, M.; Habrych, M.; Wernsdorfer, W.; Abboud, K. A.; Christou, G. *J. Am. Chem. Soc.* **2004**, *126*, 4766.
(15) Dendrinou-Samara, C.; Alexiou, M.; Zaleski, C. M.; Kampf, J. W.; Kirk, M. L.; Kessissoglou, D. P.; Pecoraro, V. L. *Angew. Chem., Int. Ed.* **2003**, *42*, 3763.

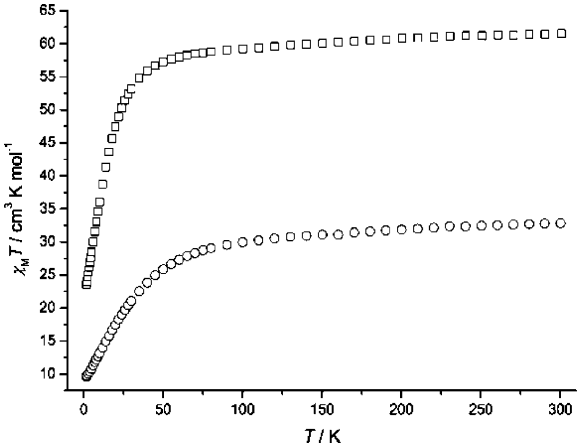

Figure 3. $\chi_M T$ vs T plots for **1**·8py·3H_2O (○) and **2**·12H_2O (□).

coordinated with square-pyramidal geometries. In all cases, the axial Mn^{III}−O bond lengths are approximately 0.20 Å longer than the equatorial Mn^{III}−O distances. Although the JT axes of Mn7 and Mn10 atoms lie almost in the same plane, a net anisotropy is expected because of the single-ion anisotropy contributions from the other Mn^{III} ions (Supporting Information).

The variable-temperature dc magnetic susceptibilities measured for the two compounds are shown in Figure 3 in the form of $\chi_M T$ versus T plots. The room temperature $\chi_M T$ values are 32.84 cm^3 K mol^{-1} for **1**·8py·3H_2O and 59.90 cm^3 K mol^{-1} for **2**·12H_2O, much lower than the expected spin-only values of 40.38 cm^3 K mol^{-1} and 71.5 cm^3 K mol^{-1} for the two compounds. $\chi_M T$ decreases continuously, upon cooling, in both cases, indicating significant antiferromagnetic interactions between the magnetic centers.

The ac magnetic susceptibility data for both **1**·8py·3H_2O and **2**·12H_2O were collected in zero-applied dc field with a 5 G ac field oscillating at frequencies in the range of 1−1500 Hz and in the temperature range of 1.8−10 K. Figure 4 shows the in-phase ($\chi_M'T$) and out-of-phase signals (χ_M'') versus T curves for complex **2**·12H_2O. This frequency-dependent response of both signals below ~*2.5 K* indicates that there is slow kinetics of magnetization reversal relative to the ac oscillation frequencies, and this is often associated with the phenomenon of single-molecule magnetism.[16] It is noticed that the $\chi'_M T$ versus T plot above 2.5 K does not display a plateau, indicating that excited states are still populated at these low temperatures.[17] Extrapolation of the $\chi'_M T$ signal from values above 3 K gives 22 cm^3 K mol^{-1} at 0 K, suggesting a spin ground state of $S = 6$ for **2**·12H_2O. The efforts to obtain the zero-field splitting parameter (D) from the $M/N\beta$ versus H/T curves, measured in the temperature range of 1.8−10 K and the dc magnetic field range of 5−70 kG, were not successful because of the population of low-lying excited states at temperatures down to 1.8 K.[18,19]

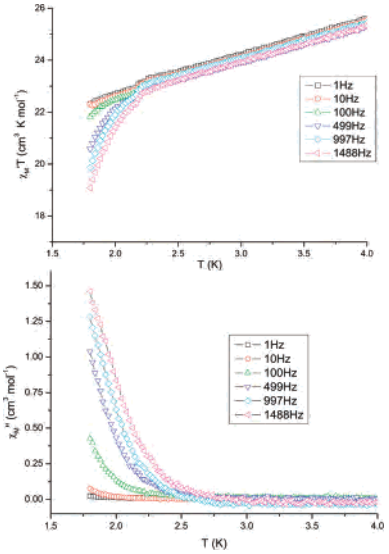

Figure 4. Plots of $\chi_M'T$ (upper) and χ_M'' (lower) versus temperature for **2**·12H_2O. χ_M' and χ_M'' are the molar in-phase and out-of-phase ac susceptibilities, respectively.

The frequency-dependent ac magnetic behavior is also observed for **1**·8py·3H_2O. In this case, extrapolation of the $\chi'_M T$ behavior to $T = 0$ K leads to a value of 9 cm^3 K mol^{-1}, corresponding to a ground state of $S = 3.5$ (Supporting Information).

In summary, two manganese phosphonate cage complexes, $[Mn^{II}Mn^{III}_{12}O_6(OH)_6(O_3PC_6H_{11})_{10}(py)_6]$ (**1**) and $[Mn^{II}_4Mn^{III}_{18}O_{12}(O_3PC_6H_{11})_8(O_2CCH_3)_{22}(H_2O)_6(py)_2]$ (**2**), are obtained simply through the change of the reaction solvents. As far as we are aware, complex **1** is the first carboxylate-free manganese phosphonate cluster, while compound **2** appears to be the largest manganese cluster thus far containing phosphonate ligand. Although both complexes display slow relaxation behaviors at low temperature, more evidence is required to determine if they are SMMs. Further work is in progress to obtain new manganese phosphonate clusters by modification of the organic groups of the phosphonate ligand.

Acknowledgment. We thank the NSFC (20325103, 20631030) and the specialized research fund for the doctoral program of the Ministry of Education of China (20040284004) for financial supports.

Supporting Information Available: Crystallographic files in CIF format, experimental procedure, four tables, and five figures. This material is available free of charge via the Internet at http://pubs.acs.org.

IC070104B

(16) Rumberger, E. M.; Shah, S. J.; Beedle, C. C.; Zakharov, L. N.; Rheingold, A. L.; Hendrickson, D. N. *Inorg. Chem.* **2005**, *44*, 2742.
(17) Boskovic, C.; Brechin, E. K.; Streib, W. E.; Folting, K.; Bollinger, J. C.; Hendrickson, D. N.; Christou, G. *J. Am. Chem. Soc.* **2002**, *124*, 3725.
(18) Murugesu, M.; Raftery, J.; Wernsdorfer, W.; Christou, G.; Brechin, E. K. *Inorg. Chem.* **2004**, *43*, 4203.
(19) (a) Rajaraman, G.; Murugesu, M.; Sanudo, E. C.; Soler, M.; Wernsdorfer, W.; Helliwell, M.; Muryn, C.; Raftery, J.; Teat, S. J.; Christou, G.; Brechin, E. K. *J. Am. Chem. Soc.* **2004**, *126*, 15445. (b) Sañudo, E. C.; Wernsdorfer, W.; Abboud, K. A.; Christou, G. *Inorg. Chem.* **2004**, *43*, 4137. (c) Scott, R. T. W.; Milios, C. J.; Vinslava, A.; Lifford, D.; Parsons, S.; Wernsdorfer, W.; Christou, G.; Brechin, E. K. *Dalton Trans.* **2006**, 3161.
(20) *SHELXTL*, version 5.0; Siemens Industrial Automation, Analytical Instrumentation: Madison, WI, 1995.